HISTONE METHYLTRANSFERASE 1 REGULATES THE ENCYSTATION PROCESS IN THE PARASITE *Giardia lamblia*

Agostina Salusso[1♦], Natacha Zlocowski[1♦], Gonzalo Mayol[1], Nahuel Zamponi[1], and Andrea S. Rópolo[1*]

[1]Instituto de Investigación Médica Mercedes y Martín Ferreyra, INIMEC – Consejo Nacional de Investigaciones Científicas y Técnicas (CONICET), Universidad Nacional de Córdoba, Córdoba, Argentina.

Article type : Original Articles

[*]**Corresponding author:** Andrea Silvana Rópolo, Instituto de Investigación Médica Mercedes y Martín Ferreyra, INIMEC (CONICET), UNIVERSIDAD NACIONAL DE CORDOBA. Friuli 2434, 5000, Córdoba, Argentina. Phone-fax: (54) (351) 468-1465/ 54-351-4695163. Email: aropolo@immf.uncor.edu

♦ These authors contributed equally to this work and should be considered co-first authors.

Running title: HMT-1 during *Giardia* differentiation.

Abbreviations: PTM (posttranslational modifications), HMT (histone methyltransferase), GlHMT1 (giardial histone methyltransferase 1), CWPs (cyst wall proteins), SET (SU(var)3-9, Enhancer-of-Zeste, Trithorax), NLS (nuclear localization signal); WT (wild type), HAT (histone acetyltransferase); HDAC (histone deacetylase); h.p.i (hours post-induction); SAM (S-adenosyl-L-methionine); ESV (encystation specific vesicles).

Keywords: epigenetic, methylation, cysts, Giardia, parasite.

Conflicts of interest: The authors declare that they have no competing interests.

ABSTRACT

In eukaryotes, histone lysine methylation is associated with either active or repressed chromatin states, depending on the status of methylation. Even when the amino-terminus of *Giardia lamblia* histones diverges from other organisms, these regions contain lysine residues that are potential targets for methylation. When we examined the role of the histone methyltransferase 1 (HMT1) in the regulation of the encystation process by GlHMT1 overexpression or downregulation, we observed an increase or a decrease of cyst production respectively, compared to wild-type trophozoites. A time-lapse analysis of encystation showed that overexpression of GlHMT1 induced an earlier and faster process than in wild-type cells together with an upregulation of mRNA expression of cyst wall proteins. Subcellular localization studies indicated that GlHMT1-HA was mainly associated with the nuclear and perinuclear region in both growing and encysting parasites, in agreement with bioinformatics analyses showing that GlHMT-1 possesses nuclear localization signals in addition to the classical SET and post-SET domains. Altogether, these findings suggest that the function of HMT1 is critical for the success and timing of the encystation process, and reinforce the idea that epigenetic marks are critical for cyst formation in *G. lamblia*.

INTRODUCTION

One major contributor to gene expression dynamics is chromatin, primarily composed of the nucleosome core, a structure of DNA wrapped around a histone octamer, formed by two monomers of each histone (H2A, H2B, H3 and H4) and a copy of linker histone H1. N-terminal histone tails vary between 10 and 35 amino acids in length and protrude from the nucleosome core. These are major sites of posttranslational modifications (PTMs), including acetylation, methylation, phosphorylation, SUMOylation, ubiquitination and deimination,

among others [1, 2]. These PTMs of histones partially regulate access to information contained in the DNA, increasing the biochemical diversity that regulates chromatin structure and function. Research in this field during recent years has focused on defining the distribution, biochemistry and cellular function of individual or of combinations of PTMs of histones. The idea that distinct downstream events can be directed by histone modification and delivered by the chromatin remodeling complex is known as the “histone code”, and the histone modifying enzymes are considered to be the writers of the histone code [2, 3].

Histone methyltransferases (HMT) catalyze the addition of methyl groups to lysine or arginine residues in the N-terminal of histones H3 and H4. The lysine residue can be mono-, di- or tri-methylated and the arginine residue can be only mono- or di-methylated. The final result of the incorporation of a methylated group is variable, from transcriptional activation to silencing, depending on the particular target residue and the particular histone. There are two groups of histone lysine methyltransferases, and both use S-adenosyl-L-methionine (SAM) as a methyl donor. The first one groups enzymes characterized by having a conserved SET (SU(var)3-9, Enhancer-of-Zeste, Trithorax) domain, consisting of approximately 130 amino acids, and is responsible for the catalytic activity of these methyltransferases. The evolutionarily conserved SET domain carries four conserved motifs: GXG, YXG, NHXCXPN and ELXFDY. Also, it was described the presence of two closely packed cysteine-rich modules: the pre-SET, which is important to maintain structural stability, and the post-SET, which is part of the active site lysine channel [4].

Some evidence of PTMs has already been described in the protozoan *Giardia lamblia* [5-8]. This is a parasite that infects humans and other vertebrates and is the causative agent of giardiasis [9]. Its life cycle is simple, with two clearly differentiated forms: the trophozoite, which inhabits the small intestine of the host and is responsible for the clinical manifestation of the disease; and the cyst, which is the infective stage. The conversion of trophozoites to cysts occurs in the lower parts of the small intestine and requires significant changes in cell structure and complex regulation at the gene and protein level. During this process, called

encystation, cyst wall proteins (CWPs) are de novo synthesized and are transported by encystation-specific vesicles (ESV) to the cell surface. In recent years, there has been much research to disclose the mechanisms underlying this tightly coordinated process, which involves early and late phases. Cholesterol deprivation was observed to be sufficient and necessary to trigger the differentiation of trophozoites into cysts [10]. Also, several transcriptional factors were observed to be upregulated during encystation, with Myb-like transcription factor being a main factor regulating the encystation-specific genes. It was demonstrated that *myb1-like protein* expression is induced early during encystation and that it interacts with double-stranded DNA and is able to bind to a particular domain present in the 5'-flanking region of the encystation-induced genes (cwp1, cwp2, cwp3, g6pi-b) and to itself [11-13]. Recently, the changes in gene expression profile during the encystation process have been studied by RNA-seq, showing similar temporal patterns in the expression of many known and putative transcriptional factors and transcription repressors, as well as histone modifiers, such as histone methyltransferases (HMTs), histone deacetylases (HDACs) and histone acetyl-transferases (HATs) [14]. The importance of the acetylation/deacetylation of histones during encystation was demonstrated using an HDAC inhibitor (FR235222), showing that the decrease of histone acetylation is critical for cyst formation, and pointing up the importance of epigenetic regulation mechanisms during encystation [5]. Also, GlSIR2.2 (GL50803_10707) was described as a SIRT1 homolog with NAD^+-dependent deacetylase activity. Although a substrate for GlSIR2.2 was not found, the enzyme was located in the nuclei [7]. In a recent report, some HAT and HDAC were described and their function explored during encystation [8]. The authors conclude that the deacetylation of histones is likely related to *cwps* gene expression, confirming the results found by Sonda et al [8]. Although histone lysine methylation is an epigenetic mark involved in many critical cellular processes, few studies were conducted in *Giardia lamblia.* Evidence of histone methylation was reported, using commercial antibodies against some histone modifications, and using immunofluorescence to analyze substrate localization [8, 15]. Although mono-, di- and tri-methylation of the H3K4 were described in the parasite, as well

as the tri-methylation of H3K9, showing marks distributed in the nuclei, there are no reports related to the enzymes involved in this process. In this work, we made a complete analysis of one of the histone methyltransferases present in *G. lamblia*. Using bioinformatics, molecular and cellular biology studies and overexpression or downregulation of the GlHMT1, we conclude that GlHMT1 is a key enzyme during the encystation process, involved in early upregulation of the genes related to cyst wall formation, supporting the idea that epigenetic marks are critical during the encystation process in *G. lamblia*.

RESULTS

Giardial HMT-1

Analysis of the *Giardia* Genome Database (http://giardiadb.org) revealed the presence of three putative histone methyltransferases in all the annotated assemblages of *G. lamblia* (Table 1). To confirm the presence of putative giardial HMTs, a HMMER search was performed against the complete proteome of *Giardia*, using a SET HMMs profile from Pfam. Since histone methyltransferases contain a classical catalytic SET domain, the search was made taking into consideration all described proteins containing SET domains and known catalytic activity demonstrated at the experimental level. All the giardial sequences found (Table 1) were located in different clades, together with proteins from *Homo sapiens*, *Mus musculus*, *Drosophila melanogaster*, *Saccharomyces cerevisiae*, *Toxoplasma gondii*, *Cryptosporidium parvum*, among others (Figure 1A). We analyze the identity (I) as well as the similarity (S) of amino acids between the putative GlHMTs with its closest homologous and we found for GlHMT1 39% (I) and 59% (S), 23% (I) and 70% (S) for GlHMT2 and 35% (I) and 59% (S) for GlSET-2. Also, it is possible to predict the function of putative proteins using information from sequences in the same cluster. Interestingly, GlHMT1 shares a clade with proteins that methylate the Lys 36 of Histone H3 (Figure 1B), GlHMT2 is located together with proteins that methylate the Lys 9 of Histone H3, while GlSET-2 is in a clade in which most proteins show methylation of Lys 4 of Histone H4.

Recently, Einarsson et al., characterized the periodicity of gene expression during the encystation process, and found that the chromatin modifier GlHMT1 is upregulated during the differentiation of the parasite [14]. Therefore, we focus our studies in this enzyme, and decided to make a complete bioinformatics analysis as well as cellular and molecular studies during the encystation of the parasite. Multiple sequence alignment of select members of the SET domain family showed a high level of sequence similarity between GlHMT1 and histone methyltransferases from different species (Figure 2A). The classical catalytic SET domain, characterized by the presence of four conserved motifs (GXG, YXG, NHXCXPN and ELXFDY), which forms the active site, as well as the cysteine-rich region (post-SET), are conserved in all *Giardia* assemblages (Figure 2B). A 3D model of GlHMT1 was built and compared by structural alignment with the resolved structure of the human ASH1 obtained from the Protein Data Bank (3OPE), showing high overlap between homolog structures (Figure 2C).

We analyzed the predicted protein-protein interaction network of GlHMT1 to search for putative direct partners (Figure 2D) of GlHMT1. In accordance with what is known for many GlHMT1 homologs, a DNA-directed RNA polymerase (GlRBP1-3), part of the complex that catalyzes RNA synthesis using DNA as a template, was found in the network. Also, we found that GlHMT1 interacted with HDAC (NAD+ independent deacetylase) and with HMT2, two chromatin modifiers that may be involved in GlHMT1 regulation.

.

Giardia HMT1 during growth

Localization studies were performed in WB-strain transgenic trophozoites, which stably expressed HMT1 containing three hemaglutinin (HA) epitope sequences at the C-terminus both under the tubulin promoter (*glhmt1-ha*), or under the endogenous promoter (*glehmt1-ha*). Over-expression of HMT1-HA showed nuclear as well as perinuclear and cytoplasmic localization by immunofluorescence assays (IFA) and confocal microscopy (Figure 3A). Under its endogenous promoter, eHMT1-HA showed a similar pattern, although the label was more discrete, showing mainly perinuclear localization in clusters or around each

nucleus. Nuclear localization, overlapping with DAPI-stained DNA, is expected for labeled histones, and the staining of both nuclei suggests that all the chromatin may be modified by this enzyme. The nuclear localization of GlHMT1 is consistent with the presence of NLS in its sequence (Figure 2A).

We performed growth curves to analyze whether GlHMT1 overexpression produced any alteration to cell growth. As shown in Figure 3B, no significant effect was observed in cell growth in *glhmt1-ha* or *glehmt1-ha* transfected cells compared to wild-type trophozoites. This suggests that methylation may not play a critical role during *Giardia lamblia* growth.

Giardia HMT1 during encystation

Previous results have suggested that some epigenetic modifications, such as acetylation and methylation, may be involved in encystation and cyst formation [5, 8]. Moreover, during encystation, a periodic pattern was found in the expression of histone deacetylase, histone methyl transferase and histone acetyl transferase genes [14]. Using our encystation protocol, we performed the analysis of the temporal expression of GlHMT1 by qRT-PCR (Figure 4A). We found that there was a significant increase in mRNA expression of *hmt1* as early as 6 h after the induction of the encystation (h.p.i.) process, but the expression values dropped after 24 h. This finding suggests a possible role of GlHMT1 at the beginning of the encystation process. When we analyzed the number of cysts produced, we found that, after 36 h.p.i., the number of cysts was significantly higher in *glhmt1-ha* transfected cells than in wild-type trophozoites, and this difference was even greater after 48 h.p.i. (Figure 4B). Interestingly, during the whole process, the localization of the enzyme was similar to that found during the growing phase and no colocalization with specific encystation vesicles (ESVs) was observed (Manders: 0.53 ± 0.8).

In order to understand the involvement of GlHMT1 in encystation, we quantified its expression in growing trophozoites (T), early encysting cells (E1), late encysting cells (E2) and cysts (C), using an antibody against one of the proteins involved in cyst wall formation (CWP1) as monitor of the progression of the process. E1 correspond to encysting parasites

with a small number and size of ESVs containing CWP1, E2 correspond to encysting parasites with larger ESVs, and C to forming or formed cysts with CWP1 labeling the surface of the cell. We found that transgenic *glhmt1-ha* trophozoites had more cells in the E1 stage at 24 h.p.i. than wild-type cells (Figure 5A). This finding was more evident after 36 h.p.i., at which most cells in *glhmt1-ha* transfected cells were in E1 and E2, while in wild-types the majority of the cells were in the T stage (Figure 5B). Finally, after 48 h.p.i., more cysts were produced in *glhmt1-ha* cells than in wild-types, similar to what was observed in Figure 4B (Figure 5C). Therefore, we concluded that GlHMT1 has a critical role during the encystation process in the regulation of CWP expression and cyst production.

To further test our findings, we analyzed whether the increase in cyst production was correlated with an increase in the abundance of mRNA transcripts of the CWPs, which are the main proteins that form the cyst wall, and the transcriptional factor Myb1-like protein, which has been indicated as a key regulator of the encystation process. We performed qRT-PCR in *glhmt1-ha* and *wild type* cells and expressed the changes in mRNA abundance as the ratio between transcript levels in *glhmt1-ha* and *wild type* cells. We observed that the kinetics of CWP1 mRNA expression showed a peak very early during encystation, similar to Myb1-like protein (Figure 6). On the other hand, CWP2 and CWP3 showed increases in their expression after 6 h.p.i. and 12 h.p.i. respectively. At 24 h.p.i., the expression of all the proteins decreased, matching the protein downregulation necessary to complete the encystation process of the parasite.

HMT1 downregulation and encystation

In order to confirm our findings regarding the role of GlHMT1 during the encystation process, we downregulated the enzyme by expressing the antisense sequence of the gene (*glhmt1-as*). We evaluated the expression of *hmt1* in transgenic glhmt1-as trophozoites and we found a clear downregulation in the expression of the glhmt1 gene compared to wild-type cells (Figure 7A). When we induced the encystation process and evaluated the cyst production after 48 h.p.i., we found significant differences between *glhmt1-as* and *wild-type*

cells (Figure 7B). Also, we counted the number of ESVs/cells during early stages of the encystation process, and we found a lower number of ESVs/cells in glhmt1-as cells compared to wild type trophozoites (Figure 7C). Finally, we assessed the differences in mRNA abundance of *CWP1-3* and *Myb1-like protein* in glhmt1-as cells and we found a downregulation of each mRNA at different time-points of encystation compared to *wild type* cells. Thus, when the expression of GlHMT1 is reduced, a clear downregulation of the encystation process occurs, supporting that GlHMT1 is involved in the upregulation of encystation-specific genes during early stages of the encystation process.

DISCUSSION

To complete its life cycle, *Giardia lamblia* must differentiate from a motile form to a dormant cyst stage, a process that requires a refined system to regulate gene expression in response to different stimuli and changes in its environment. It is now known that many of these changes are achieved via post-translational modifications in histones that influence gene expression. In this manuscript, we described GlHMT1 as a key enzyme involved in cyst formation, adding new insights in the epigenetic control of the encystation process.

Gene expression in *Giardia* is dynamic, with a considerable number of genes, like *cwp1-3*, exclusively expressed during the encystation process, and others that are upregulated during this process, like the transcriptional factor *Myb1-like protein*. Also, other transcriptional factors were described whose expression increased significantly during encystation, like ARID1, GARP-like protein and WRKY [16-18]. We found that the expression of GlHMT1 is upregulated early during the encystation process, with a peak between 6 and 12 h.p.i., later returning to basal levels in wild-type cells. Also, in overexpressing glhmt1 cells, the rise of the transcriptional factor Myb1-like protein was as early as 6 h.p.i., and then we found the increase in the mRNA levels of the cwp mRNA, matching previous results in which an increase in the expression of transcriptional factors was described in the early stages of the process. Recently, Einarsson et al. described the temporality of gene expression during encystation [14]. They used, instead of the classical

two step encystation protocol, a new one in order to obtain higher levels of mature cysts, and then they studied the total gene expression profiles during the complete encystation process using RNA-seq. They found that most of the histone modifying enzymes (HAT, HDAC and HMT) were upregulated late during the encystation process (22-32 hours) as well as the transcriptional factors WRKY, and that myb1-like and myb1 shown the higher increase at 7h and 22hs respectively. Considering the differences in the encystation protocols and the use of different *G. lamblia* isolates (WB clone 1267 in our study and WB clone C6 in Einarsson et al.), it seems that the linear progression of the process is the same in both conditions, with an early upregulation of myb1-like protein, and then the upregulation of chromatin modifiers.

The cellular panorama of lysine methylation provides contrasting functional effects, ranging from silencing to activating target genes (reviewed in [4, 19]). Here, we found a clear upregulation of the encystation process in *Giardia* cells overexpressing GlHMT1. However, we did not explore experimentally the substrate of the enzyme. The presence of mono-, di- and tri-methylation of H3K4 and H3K9 tri-methylation have been demonstrated in this parasite using commercial antibodies, providing further evidence of the possible function performed by these enzymes [8]. Moreover, in other eukaryotic cells, it is well known that the same HMT can have multiple substrates, including non-histones. Therefore, although bioinformatics data gives an idea of the putative substrate of HMT1, this enzyme as well as HMT2 and SET-2 may have many targets. Further experiments using mass spectrometry, commercial antibodies and in vitro activity assays may help to start to disclose the target/s of these enzymes.

In eukaryotic cells, most histone modifications have been found to be reversible, and the enzymes that remove this modification have been described. Histone lysine methylation can also be reversed by two families of enzymes, amino oxidases such as LSD1 (remove mono- and dimethyl lysines) and hydroxylases of the JmjC family (remove mono-, di- and trimethylated lysine) [19]. An interesting feature of *G. lamblia* is that it has no demethylases in its genome, suggesting that this modification might be irreversible in the parasite. However, before discarding the possibility of reversibility, a complex bioinformatics study to

identify putative enzymes should be carried out, taking into account the low similarities between the amino acid composition of giardial sequences and those of other groups of eukaryotes. Also, the absence of arginine methyltransferases in the *Giardia* genome is intriguing. Mass spectrometry studies of histones during growth and encystation will help to unravel the histone modifications and will also give an idea of the particularities at each stage of the parasite's life cycle.

The only known stimulus that triggers encystation is the lack of cholesterol, a typical feature of the lower parts of the intestine [10]. It has been suggested that the trophozoites sense this difference in cholesterol concentration, triggering the encystation process. However, the link between the lack of cholesterol and the transcriptional activation of specific genes is still incomplete. From the analysis of the predicted protein-protein interaction network of GlHMT1, we found a possible interaction of GlHMT1 with HDAC (NAD+ independent deacetylase). It was observed that classical inhibitors of HDAC (FR235222, Trichostatin A and Sodium Butyrate) reduce the encystation process in *Giardia lamblia* by inhibiting the expression of encystation-specific molecules [5, 8]. In mammalian cells, an interplay between acetylation, deacetylation and the activity of a HMT has been described [20]. It was found that the enzymatic activity of the enzyme SUV39H1 (lysine methyltransferase) is negatively regulated by acetylation at residue Lys 266, and that SIRT1-mediated deacetylation relieves this inhibition. Also, the Lys 266 is located in an exposed loop that participates in mediating the interaction between the SET domain and the cysteine-rich post-SET domain [20]. The authors propose that acetylation of Lys266 could alter this inter-domain interaction and affect the specific activity of the enzyme, explaining the stimulatory effect of Lys266 deacetylation on SUV39H1 activity. We explored whether GlHMT1 may possess putative acetylation sites in its SET domain, finding that the Lys220 is a possible site of acetylation. This lysine is located in an exposed loop near the post-SET domain (Figure 8). Therefore, it may be possible to explain the action of the HDAC inhibitors by a

dual function: deacetylation of particular sites of histones, and a GlHMT1 activity regulator. Studies regarding Lys220 mutation are being conducted to test this possibility.

HDAC and HMT inhibitors are emerging treatments for cancer, and the HDAC inhibitor vorinostat has been approved for use in cutaneous T cell lymphoma, while others are in clinical trials (reviewed in [21-24]. Considering that differentiation from the trophozoite into cyst is critical for parasite survival in the environment and for disease transmission, the finding of the key regulator GlHMT1 during the early phase of encystation clearly illuminates the idea of the use of HMT inhibitors to effectively block the production of *Giardia* cysts and thus reduce disease transmission.

EXPERIMENTAL PROCEDURES

Parasites:

Trophozoites of the isolate WB, clone 1267 (American Type Culture Collection 50582) were axenically cultivated in screw cap borosilicate glass tubes in modified TYI-S-33 medium enriched with 10% heat-inactivated fetal bovine serum at pH 7.5 supplemented with 0.1% bovine bile for 72 hours at 37ºC. Cultures were harvested by chilling on ice followed by agitation to dislodge attached cells. Trophozoites were collected by centrifugation at 500 x g for 10 min at 4ºC and washed three times with PBS [25]. A two-step encystation procedure was used by increasing the medium pH and adding porcine bile, as reported by Boucher and Gillin [26].

Expression of HMT1 and eHMT1 in WB/1267 trophozoites

Wild-type trophozoites (WB/1267) were used as hosts for the expression of transgenic genes and as wild-type controls. The GlHMT1 open reading frame was amplified from genomic DNA using the f1 (5'CATTCCATGGGCAAAGTAATGGCAATGAAG) and r1 (5'CATTGATATCTGTCCTTAACTTTGGTGCATC) primers and cloned into the plasmid pTubHAc-pac [22] with HA at the C-terminus to generate the pHMT1-HA episomal vector. To express the endogenous HMT1p, the eHMT1-HA vector was constructed by replacing the

tubulin promoter of HMT1-HA by a sequence containing the putative *hmt1* endogenous promoter, using the primers f2 (5'CATTTCTAGACGATGAATTCGTGAAATCTCTTG) and r1. The entire open reading frame was sequenced (Macrogen). The vector contains a puromycin cassette under the control of the endogenous non-regulated tubulin promoter, for cell selection. Stable episomal trophozoite transfection was performed by electroporation as previously described [27-30]. For HMT1 antisense, the entire sequence of the ORF was amplified using the ASf (5'CATTCCATGGTATAATCGAAGCTAAGCTCTTCA) and ASr (5' CATTGATATCATGGGCAAAGTAATGGCAATGAAG) primers, restricted and ligated to the pTubHAc-pac in the opposite direction, resulting in the antisense vector that was used for inhibition of HMT1 expression.

Datamining, phylogenetic and structural analysis.

The complete proteomes of *Cryptosporidium parvum*, *Plasmodium falciparum*, *Toxoplasma gondii*, *Trichomonas vaginalis*, *Trypanosoma cruzi* and *Giardia lamblia* assemblages A, A*2*, B, B*2* and E were downloaded. The Hidden Markov Model for SET

domains (PF00856) was obtained from Pfam (www.pfam.xfam.org) [31]. Sequences containing the SET domain were gathered by using the HMMER [32]. Both searches were performed with default settings. 196 sequences were obtained and each one was scanned with Prosite and Pfam servers (http://prosite.expasy.org/) to find specific signals and domains (Supplementary Table 1). Multiple sequence alignment was carried out with the on-line version of MAFFT (http://mafft.cbrc.jp/alignment/server/) with default settings and manual curation was performed [33, 34].

The phylogenetic tree was built by Maximum Likelihood (ML) using PhyML [35]. with approximate likelihood-ratio test (aLRT) and a bootstrap number of 100 and default settings. Sequences were clustered in monophyletic groups. Only those groups with > 10 sequences were considered. The clustering was analyzed by HMMerCTTer (http://lidecc.cs.uns.edu.ar/cab2c2015/proceedings/handle/1234/127) and SDPfox (http://bioinf.fbb.msu.ru/SDPfoxWeb/main.jsp) [36]. The maximum allowed percent of gaps

was set at 90%, resulting in six well-defined groups. The phylogenetic tree was edited with iTOL (http://itol.embl.de/) [37].

Structural analysis was performed by predicting the 3D structure of the protein codified by the gene GL50803_9130 using three servers, I-TASSER (http://zhanglab.ccmb.med.umich.edu/I-TASSER) [38, 39], Phyre2 (http://www.sbg.bio.ic.ac.uk/~phyre2/html/page.cgi?id=index) [40] and RaptorX (http://raptorx.uchicago.edu/) [41]. The VMD program was used for the visualization of these structures as well as to generate 3D alignment, besides the RaptorX server [42-44]. The structure of ASH1L was obtained from the Protein Data Bank (http://www.rcsb.org/pdb/home/home.do) under the id 3OPE [45]. The prediction of NLS was carried out by the cNLS Mapper (http://nls-mapper.iab.keio.ac.jp/cgi-bin/NLS_Mapper_form.cgi) and NucPred (https://www.sbc.su.se/~maccallr/nucpred/cgi-bin/single.cgi) [46, 47].

Co-evolution analysis was performed by MISTIC (http://mistic.leloir.org.ar/index.php) under default settings with the structure obtained from I-TASSER and the sequence of GL50803_9130 first at the MSA [48].

HMT1 protein-protein interacting partners were predicted by combining the Interlogog approach (Zamponi N *et al.*, unpublished results) and information retrieved from the STRING database. Only experimentally validated interactions with scores above 900 were considered (STRING v10: protein-protein interaction networks, integrated over the tree of life).

Immunofluorescence

Cells were washed with PBSm (1% growth medium in PBS, pH 7.4), allowed to attach to glass slides for 1 h at 37ºC in a humidified chamber and then fixed with fresh 4% formaldehyde for 40 min at room temperature. Cells were incubated with blocking solution (10% goat serum and 0.1% Triton X-100 in PBS) at 37ºC for 60 min. For direct immunofluorescence, FITC conjugated mAb anti-HA (1:100; Sigma-Aldrich, St. Louis, MO) or FITC conjugated anti-CWP1 mouse mAb (1:200; Water-borne, New Orleans, LA, USA)

were used. For double staining, cells were first incubated with anti-HA mAb (1:300; Sigma-Aldrich, St. Louis, MO) followed by incubation with Alexa 546 goat anti-mouse (1:500; Termo Fisher Scientific Inc.). All incubations were made during 1 h at 37ºC in a humidified chamber. Controls with an unrelated antibody were included. Fluorescence staining was visualized with a motorized FV1000 Olympus confocal microscope (Olympus UK Ltd, UK) using 63X oil immersion objectives (NA 1.32, zoomX). Differential interference contrast images were collected simultaneously with the fluorescence images by the use of a transmitted light detector. Images were processed using ImageJ and Adobe Photoshop 8.0 (Adobe System) software. For quantitative studies, all images of a given experiment were exposed and processed identically. At least 100 cells expressing each type of protein were examined.

Quantitative colocalization analysis (QCA)

Confocal immunofluorescence microscopy and quantitative colocalization analysis were performed using Fiji image processing package (http://fiji.sc/wiki/index.php/Fiji). Background was corrected using the threshold value for all channels to remove background and noise levels completely. The Manders (M) overlap coefficient was examined. The M values range from 0 to 1.0. If the image has an overlap coefficient of 0.5, it implies that 50% of both its objects, i.e. pixels, overlap. A value of zero means that there are no overlapping pixels. This coefficient is not sensitive to the limitations of typical fluorescence imaging [49, 50]. Colocalization is considered in the range from 0.7 to 1.0.

Growth curves

Tubes containing 7 ml of growth medium without puromycin were inoculated with 5 x 10^5 cells/ml from logarithmic phase cultures of wild type and HMT1-HA trophozoites. Every 12 h, the tubes were chilled on ice for 20 min to detach adherent living trophozoites and the number of viable cells were determined by counting on a hemocytometer after staining with 0.4% Trypan blue, according to manufacturer's instructions (Sigma Chemical Co, USA).

Relative quantitative Real time-PCR (qRT-PCR)

Cells were homogenized in Trizol reagent (Thermo Fisher Scientific Inc.) and stored at -80ºC before total RNA extraction, using SV total RNA Isolation System (Promega, Madison, WI), according to the manufacturer's specifications. 2 µg of total RNA from each condition were reverse transcribed using Reverse Transcriptase M-MLV (Promega, Madison, WI). cDNA was analyzed for wild-type and transgenic trophozoites genes using real-time PCR SYBR Green Master Mix (Thermo Fisher Scientific Inc.), single stranded cDNA (100 ng of the imput total RNA equivalent), and 800 nM of amplification primer were used in a reaction volume of 20 µl. Specific primers were designed using Primer Express software (Applied Biosystems) for detection of the Cyst Wall Proteins, Myb1-like protein and HMT-1: cwp1realF (AACGCTCTCACAGGCTCCAT) and cwp1realR (AGGTGGAGCTCCTTGAGAAATTG); cwp2realF (TAGGCTGCTTCCCACTTTTGAG) and cwp2realR (CGGGCCCGCAAGGT); cwp3realF (GCAAATTGGATGCCAAACAA) and cwp3realR (GACTCCGATCCAGTCGCAGTA); Myb1realF (TCCCTAATGACGCCAAAC) and Myb1realR (AGCACGCAGAGGCCAAGT); HMT1realF (AAGCTGTGAGCTCAGGAAGG) and HMT1realR (CTGCGCAGCACTCTTTGTAG). Runs were performed on a standard 7500 system (Applied Biosystems). The relative-quantitative RT-PCR conditions were: 50ºC for 2 min, 95ºC for 10 min and 40 cycles at 95ºC for 15 s and 60ºC for 1 min. Gene expression was normalized to the housekeeping gene 18s (Fw AAGACCGCCTCTGTCAATAA and Rv: GTTTACGGCCGGGAATACG primers) and calculated using the comparative ΔΔCt method. Melting curve analyses were performed to ensure the specificity of the qPCR product. These assays were performed three times in duplicates.

Statistics

Results were analyzed for statistical significance by performing unpaired, two-sided Student's t-test with Graph Pad Prism 5 Data Analysis Software (GraphPad Software Inc., La Jolla, CA). Mean and standard error of mean (SEM) values were calculated from at least three biologically and technically independent experiments. $p<0.05$ was considered significative and was indicated by asterisks in figures.

ACKNOWLEDGMENTS

We thank Florencia Dadam and Dr. Carla Cisternas for useful technical assistance on qRT-PCR and Maria Carolina Touz for critical reading of the manuscript. We also thank grant support from the Agency for Promotion of Science and Techonology (ANPCYT), the National Council for Scientific and Technical Research of Argentina (CONICET) and the Secretary of Science and Technology of the National University of Cordoba (SECYT).

AUTHOR CONTRIBUTIONS

NZolowski and AS performed the experiments and analyzed the data. GM and NZamponi identified and assembled the datasets sequences and generated the phylogenetic tree and all the bioinformatics analysis. ASR conceived and designed the study, directed the research and wrote the manuscript with input from all authors. All authors read and approved the final manuscript.

REFERENCES

1. Bannister, A. J. & Kouzarides, T. (2011) Regulation of chromatin by histone modifications, *Cell Res.* **21**, 381-95.
2. Jenuwein, T. & Allis, C. D. (2001) Translating the histone code, *Science.* **293**, 1074-80.
3. Strahl, B. D. & Allis, C. D. (2000) The language of covalent histone modifications, *Nature.* **403**, 41-5.
4. Lanouette, S., Mongeon, V., Figeys, D. & Couture, J. F. (2014) The functional diversity of protein lysine methylation, *Mol Syst Biol.* **10**, 724.
5. Sonda, S., Morf, L., Bottova, I., Baetschmann, H., Rehrauer, H., Caflisch, A., Hakimi, M. A. & Hehl, A. B. (2010) Epigenetic mechanisms regulate stage differentiation in the minimized protozoan Giardia lamblia, *Mol Microbiol.* **76**, 48-67.
6. Kulakova, L., Singer, S. M., Conrad, J. & Nash, T. E. (2006) Epigenetic mechanisms are involved in the control of Giardia lamblia antigenic variation, *Mol Microbiol.* **61**, 1533-42.
7. Wang, Y. H., Zheng, G. X. & Li, Y. J. (2016) Giardia duodenalis GlSir2.2, homolog of SIRT1, is a nuclear-located and NAD(+)-dependent deacethylase, *Exp Parasitol.* **169**, 28-33.
8. Carranza, P. G., Gargantini, P. R., Prucca, C. G., Torri, A., Saura, A., Svard, S. & Lujan, H. D. (2016) Specific histone modifications play critical roles in the control of encystation and antigenic variation in the early-branching eukaryote Giardia lamblia, *Int J Biochem Cell Biol.* **81**, 32-43.
9. Adam, R. D. (2001) Biology of Giardia lamblia, *Clin Microbiol Rev.* **14**, 447-75.
10. Lujan, H. D., Mowatt, M. R., Byrd, L. G. & Nash, T. E. (1996) Cholesterol starvation induces differentiation of the intestinal parasite Giardia lamblia, *Proc Natl Acad Sci U S A.* **93**, 7628-33.

11. Sun, C. H., Palm, D., McArthur, A. G., Svard, S. G. & Gillin, F. D. (2002) A novel Myb-related protein involved in transcriptional activation of encystation genes in Giardia lamblia, *Mol Microbiol.* **46**, 971-84.
12. Yang, H., Chung, H. J., Yong, T., Lee, B. H. & Park, S. (2003) Identification of an encystation-specific transcription factor, Myb protein in Giardia lamblia, *Mol Biochem Parasitol.* **128**, 167-74.
13. Huang, Y. C., Su, L. H., Lee, G. A., Chiu, P. W., Cho, C. C., Wu, J. Y. & Sun, C. H. (2008) Regulation of cyst wall protein promoters by Myb2 in Giardia lamblia, *J Biol Chem.* **283**, 31021-9.
14. Einarsson, E., Troell, K., Hoeppner, M. P., Grabherr, M., Ribacke, U. & Svard, S. G. (2016) Coordinated Changes in Gene Expression Throughout Encystation of Giardia intestinalis, *PLoS Negl Trop Dis.* **10**, e0004571.
15. Dawson, S. C., Sagolla, M. S. & Cande, W. Z. (2007) The cenH3 histone variant defines centromeres in Giardia intestinalis, *Chromosoma.* **116**, 175-84.
16. Wang, C. H., Su, L. H. & Sun, C. H. (2007) A novel ARID/Bright-like protein involved in transcriptional activation of cyst wall protein 1 gene in Giardia lamblia, *J Biol Chem.* **282**, 8905-14.
17. Sun, C. H., Su, L. H. & Gillin, F. D. (2006) Novel plant-GARP-like transcription factors in Giardia lamblia, *Mol Biochem Parasitol.* **146**, 45-57.
18. Pan, Y. J., Cho, C. C., Kao, Y. Y. & Sun, C. H. (2009) A novel WRKY-like protein involved in transcriptional activation of cyst wall protein genes in Giardia lamblia, *J Biol Chem.* **284**, 17975-88.
19. Thinnes, C. C., England, K. S., Kawamura, A., Chowdhury, R., Schofield, C. J. & Hopkinson, R. J. (2014) Targeting histone lysine demethylases - progress, challenges, and the future, *Biochim Biophys Acta.* **1839**, 1416-32.
20. Vaquero, A., Scher, M., Erdjument-Bromage, H., Tempst, P., Serrano, L. & Reinberg, D. (2007) SIRT1 regulates the histone methyl-transferase SUV39H1 during heterochromatin formation, *Nature.* **450**, 440-4.
21. Damaskos, C., Valsami, S., Kontos, M., Spartalis, E., Kalampokas, T., Kalampokas, E., Athanasiou, A., Moris, D., Daskalopoulou, A., Davakis, S., Tsourouflis, G., Kontzoglou, K., Perrea, D., Nikiteas, N. & Dimitroulis, D. (2017) Histone Deacetylase Inhibitors: An Attractive Therapeutic Strategy Against Breast Cancer, *Anticancer Res.* **37**, 35-46.
22. Kavanaugh, S. M., White, L. A. & Kolesar, J. M. (2010) Vorinostat: A novel therapy for the treatment of cutaneous T-cell lymphoma, *Am J Health Syst Pharm.* **67**, 793-7.
23. Zhao, H., Wang, Y. & Li, H. (2015) Cancer drug discovery targeting histone methyltransferases: an update, *Curr Med Chem.* **22**, 2075-86.
24. Verma, S. K. (2015) Recent progress in the discovery of epigenetic inhibitors for the treatment of cancer, *Methods Mol Biol.* **1238**, 677-88.
25. Keister, D. B. (1983) Axenic culture of Giardia lamblia in TYI-S-33 medium supplemented with bile, *Trans R Soc Trop Med Hyg.* **77**, 487-8.
26. Boucher, S. E. & Gillin, F. D. (1990) Excystation of in vitro-derived Giardia lamblia cysts, *Infect Immun.* **58**, 3516-22.
27. Singer, S. M., Yee, J. & Nash, T. E. (1998) Episomal and integrated maintenance of foreign DNA in Giardia lamblia, *Mol Biochem Parasitol.* **92**, 59-69.
28. Yee, J. & Nash, T. E. (1995) Transient transfection and expression of firefly luciferase in Giardia lamblia, *Proc Natl Acad Sci U S A.* **92**, 5615-9.
29. Elmendorf, H. G., Singer, S. M., Pierce, J., Cowan, J. & Nash, T. E. (2001) Initiator and upstream elements in the alpha2-tubulin promoter of Giardia lamblia, *Mol Biochem Parasitol.* **113**, 157-69.
30. Merino, M. C., Zamponi, N., Vranych, C. V., Touz, M. C. & Ropolo, A. S. (2014) Identification of Giardia lamblia DHHC proteins and the role of protein S-palmitoylation in the encystation process, *PLoS Negl Trop Dis.* **8**, e2997.
31. Finn, R. D., Bateman, A., Clements, J., Coggill, P., Eberhardt, R. Y., Eddy, S. R., Heger, A., Hetherington, K., Holm, L., Mistry, J., Sonnhammer, E. L., Tate, J. & Punta, M. (2014) Pfam: the protein families database, *Nucleic Acids Res.* **42**, D222-30.

32. Finn, R. D., Clements, J. & Eddy, S. R. (2011) HMMER web server: interactive sequence similarity searching, *Nucleic Acids Res.* **39**, W29-37.
33. Katoh, K. & Standley, D. M. (2013) MAFFT multiple sequence alignment software version 7: improvements in performance and usability, *Mol Biol Evol.* **30**, 772-80.
34. Katoh, K., Misawa, K., Kuma, K. & Miyata, T. (2002) MAFFT: a novel method for rapid multiple sequence alignment based on fast Fourier transform, *Nucleic Acids Res.* **30**, 3059-66.
35. Guindon, S., Dufayard, J. F., Lefort, V., Anisimova, M., Hordijk, W. & Gascuel, O. (2010) New algorithms and methods to estimate maximum-likelihood phylogenies: assessing the performance of PhyML 3.0, *Syst Biol.* **59**, 307-21.
36. Mazin, P. V., Gelfand, M. S., Mironov, A. A., Rakhmaninova, A. B., Rubinov, A. R., Russell, R. B. & Kalinina, O. V. (2010) An automated stochastic approach to the identification of the protein specificity determinants and functional subfamilies, *Algorithms Mol Biol.* **5**, 29.
37. Letunic, I. & Bork, P. (2011) Interactive Tree Of Life v2: online annotation and display of phylogenetic trees made easy, *Nucleic Acids Res.* **39**, W475-8.
38. Yang, J., Yan, R., Roy, A., Xu, D., Poisson, J. & Zhang, Y. (2015) The I-TASSER Suite: protein structure and function prediction, *Nature methods.* **12**, 7-8.
39. Yang, J. & Zhang, Y. (2015) I-TASSER server: new development for protein structure and function predictions, *Nucleic Acids Res.* **43**, W174-81.
40. Kelley, L. A., Mezulis, S., Yates, C. M., Wass, M. N. & Sternberg, M. J. (2015) The Phyre2 web portal for protein modeling, prediction and analysis, *Nat Protoc.* **10**, 845-58.
41. Kallberg, M., Wang, H., Wang, S., Peng, J., Wang, Z., Lu, H. & Xu, J. (2012) Template-based protein structure modeling using the RaptorX web server, *Nat Protoc.* **7**, 1511-22.
42. Humphrey, W., Dalke, A. & Schulten, K. (1996) VMD: visual molecular dynamics, *J Mol Graph.* **14**, 33-8, 27-8.
43. Eargle, J., Wright, D. & Luthey-Schulten, Z. (2006) Multiple Alignment of protein structures and sequences for VMD, *Bioinformatics.* **22**, 504-6.
44. Wang, S., Peng, J. & Xu, J. (2011) Alignment of distantly related protein structures: algorithm, bound and implications to homology modeling, *Bioinformatics.* **27**, 2537-45.
45. An, S., Yeo, K. J., Jeon, Y. H. & Song, J. J. (2011) Crystal structure of the human histone methyltransferase ASH1L catalytic domain and its implications for the regulatory mechanism, *J Biol Chem.* **286**, 8369-74.
46. Kosugi, S., Hasebe, M., Tomita, M. & Yanagawa, H. (2009) Systematic identification of cell cycle-dependent yeast nucleocytoplasmic shuttling proteins by prediction of composite motifs, *Proc Natl Acad Sci U S A.* **106**, 10171-6.
47. Brameier, M., Krings, A. & MacCallum, R. M. (2007) NucPred--predicting nuclear localization of proteins, *Bioinformatics.* **23**, 1159-60.
48. Simonetti, F. L., Teppa, E., Chernomoretz, A., Nielsen, M. & Marino Buslje, C. (2013) MISTIC: Mutual information server to infer coevolution, *Nucleic Acids Res.* **41**, W8-14.
49. Zinchuk, V., Zinchuk, O. & Okada, T. (2007) Quantitative colocalization analysis of multicolor confocal immunofluorescence microscopy images: pushing pixels to explore biological phenomena, *Acta histochemica et cytochemica.* **40**, 101-11.
50. Garcia Penarrubia, P., Ferez Ruiz, X. & Galvez, J. (2005) Quantitative analysis of the factors that affect the determination of colocalization coefficients in dual-color confocal images, *IEEE transactions on image processing : a publication of the IEEE Signal Processing Society.* **14**, 1151-8.

SUPPORTING INFORMATION

Supplementary Table 1: Sequences and organisms used in phylogenetic studies

TABLES

Table 1. Putative histone-methyltransferases in *G. lamblia*

ID	DatabaseID	Assemblage	Putative Protein
gla0000154	GL50803_9130	A - isolate WB	**GlHMT1**
glaa153297	DHA2_153297	A - isolate DH	
glb0000710	GL50581_2583	B - isolate GS	
glbb152988	GSB_152988	B - isolate GS_B	
gle0003206	GLP15_1600	E - isolate P15	
gla0000335	GL50803_221691	A - isolate WB	**GlHMT2**
glaa0000335	DHA2_154382	A - isolate DH	
glb0000586	GL50581_3980	B - isolate GS	
glbb150181	GSB_150181	B - isolate GS_B	
gle0001340	GLP15_2575	E - isolate P15	
gla0005658	GL50803_8921	A - isolate WB	**GlSET-2**
glaa0008921	DHA2_8421	A - isolate DH	
glb0001645	GL50581_420	B - isolate GS	
glbb0008921	GSB_8921	B - isolate GS_B	
gle0002966	GLP15_1900	E - isolate P15	

FIGURE LEGENDS

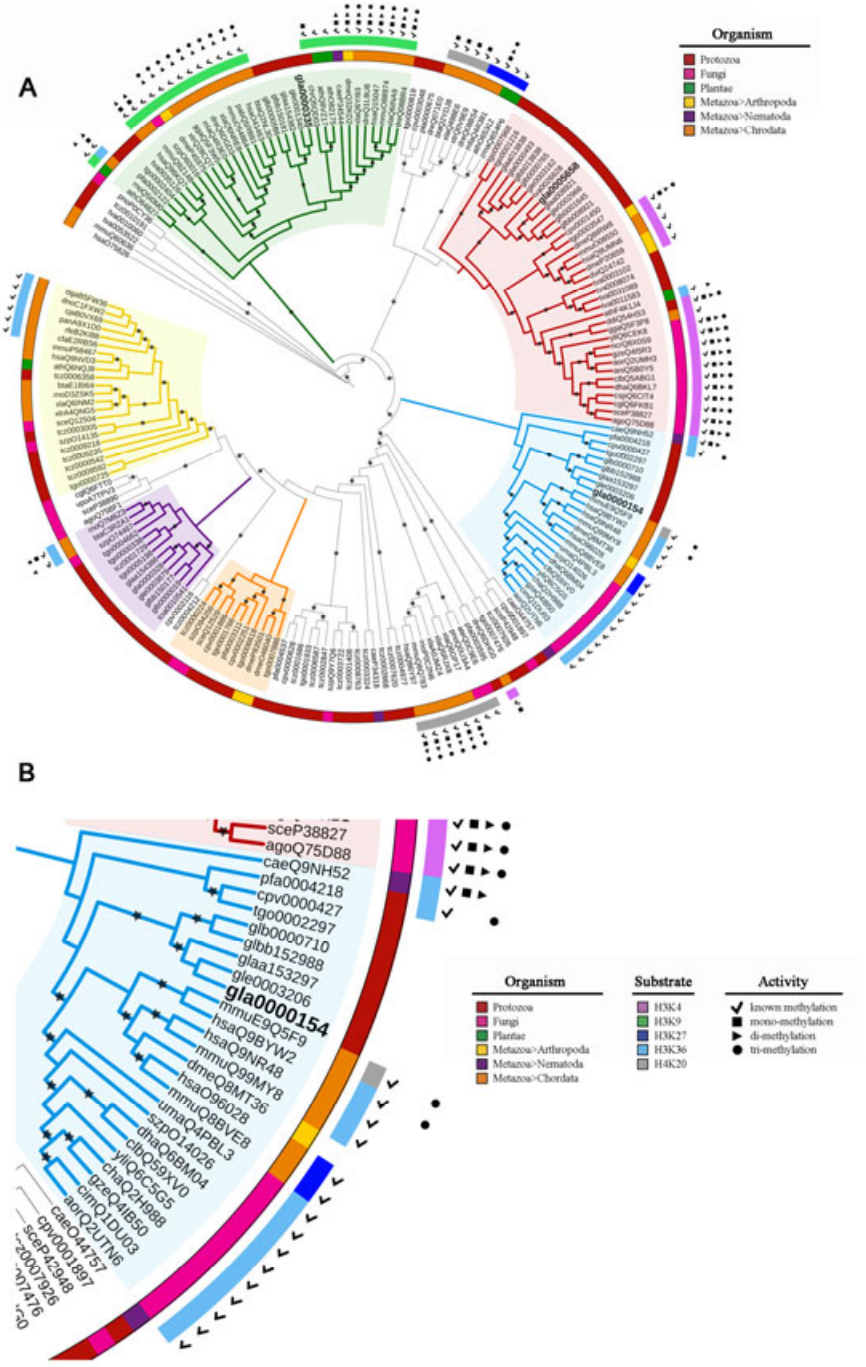

Figure 1. *Giardia lamblia* HMTs. A) The complete set of *Giardia* putative HMTs was obtained using HMMER and the SET profile from Pfam against *Giardia* proteasomes. Phylogenetic reconstruction was performed by Maximum Likelihood (ML) using PhyML with approximate likelihood-ratio test (aLRT) and 100 bootstraps. Six phylogenetically related clusters of sequences were obtained by implementing HMMerCTTer and SDPfox. Putative *Giardia* HMTs were located in different clades along the phylogenetic tree, with proteins from *Homo sapiens*, *Mus musculus*, *Drosophila melanogaster*, *Saccharomyces cerevisiae*, *Toxoplasma gondii*, *Cryptosporidium parvum* among others. **B)** *Giardia* HMT1 clustered together with histone-methyltransferases that methylate Lys 36 of Histone H3.

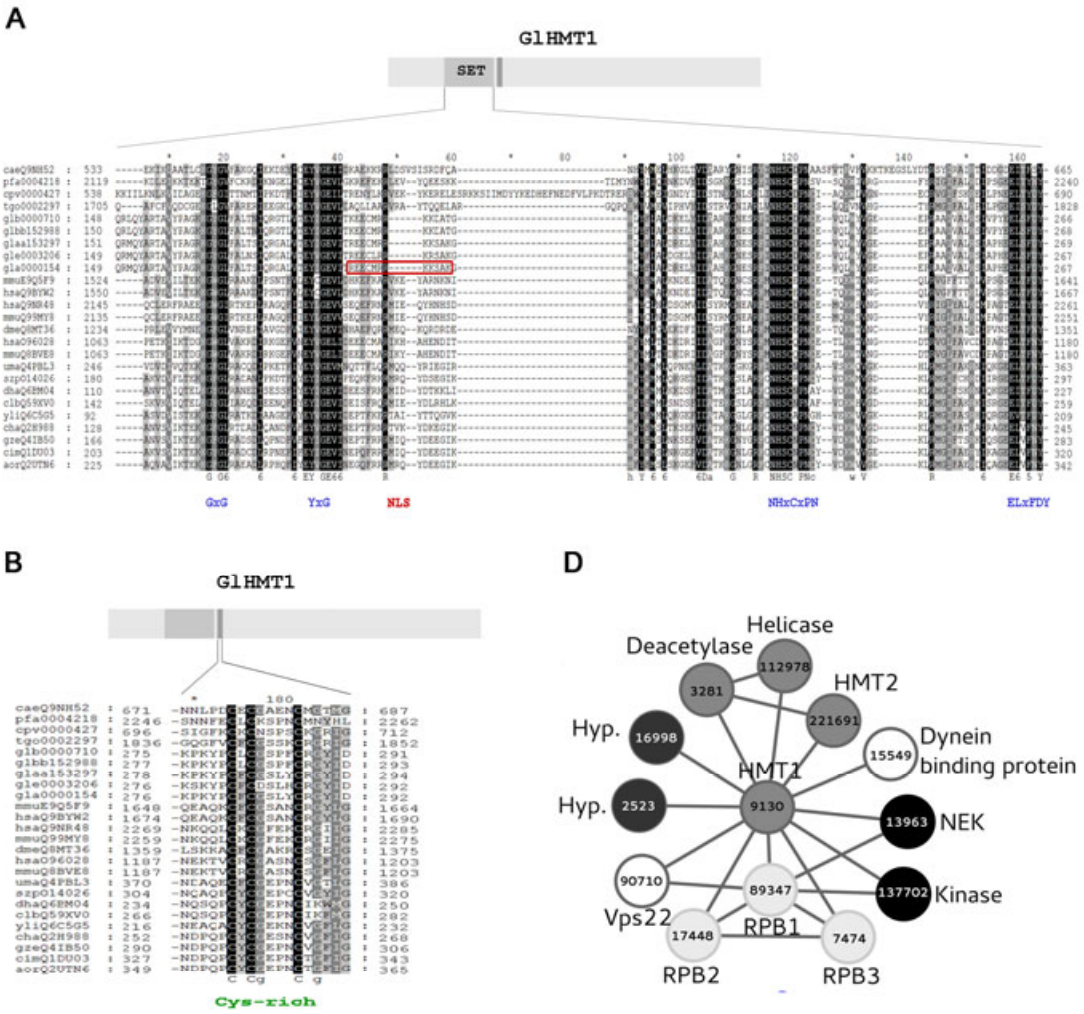

Figure 2. Characterization of *Giardia lamblia* HMT1. A-B) Alignment based on secondary structure of HMT1 from *Giardia* (Assemblages A, A2, B, B2, E) against HMT from different organisms. The SET domain (above) and the post-SET domain (below) are shown. Multiple sequence alignment was carried out with the on-line version of MAFFT with default settings. In the SET domain, the four conserved motifs (GXG, YXG, NHXCXPN, ELXFDY) that form the active sites are indicated, as well as the nuclear localization signal (NLS, rectangle in red). In the post-SET domain, the cysteine-rich region is shown. **C)** Structural analyses were performed by predicting the 3D structure of the protein codified by the gene GL50803_9130 using three servers, I-TASSER, Phyre2 and RaptorX. The VMD program was used for visualization of these structures as well as to generate 3D alignment, besides the RaptorX server. The prediction of NLS was carried out by cNLS Mapper and NucPred. In lower panels the structure of GlHMT1 (in purple) was aligned with the structure of ASH1L (in cyan), obtained from Protein Data Bank under the id 3OPE. **D)** GlHMT1 protein-protein interacting partners were predicted by combining the Interolog approach [Zamponi N et al., unpublished results] and information retrieved from the STRING database (only experimentally validated interactions with scores above 900 were considered) [STRING v10: protein–protein interaction networks, integrated over the tree of life].

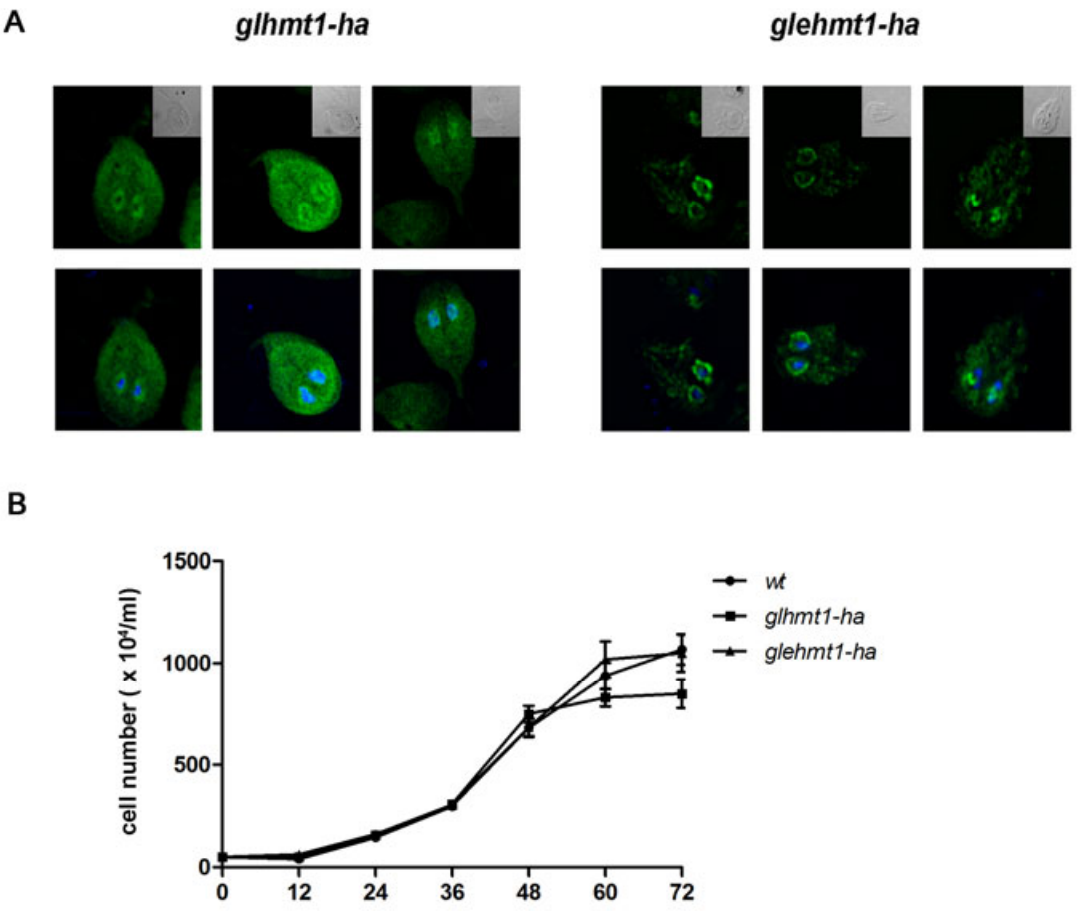

Figure 3. *Giardia* HMT1 during growth. A) Immunofluorescence assays and confocal microscopy were performed using Alexa 588-conjugated anti-HAmAb (green) in growing *glhmt1-ha* and *glehmt1-ha* transfected trophozoites. GlHMT1 mainly localized in the nuclei of the trophozoites. Nuclei were stained with DAPI (blue). Differential interference contrast images are shown as insets. **B)** *Wild type* (*wt*) and *glhmt1-ha* or *glehmt1-ha* transfected trophozoites (5 x 10^5 trophozoites) were inoculated to growth medium and the number of viable cells was determined every 12 hours using trypan blue. No differences in growth were observed between both groups.

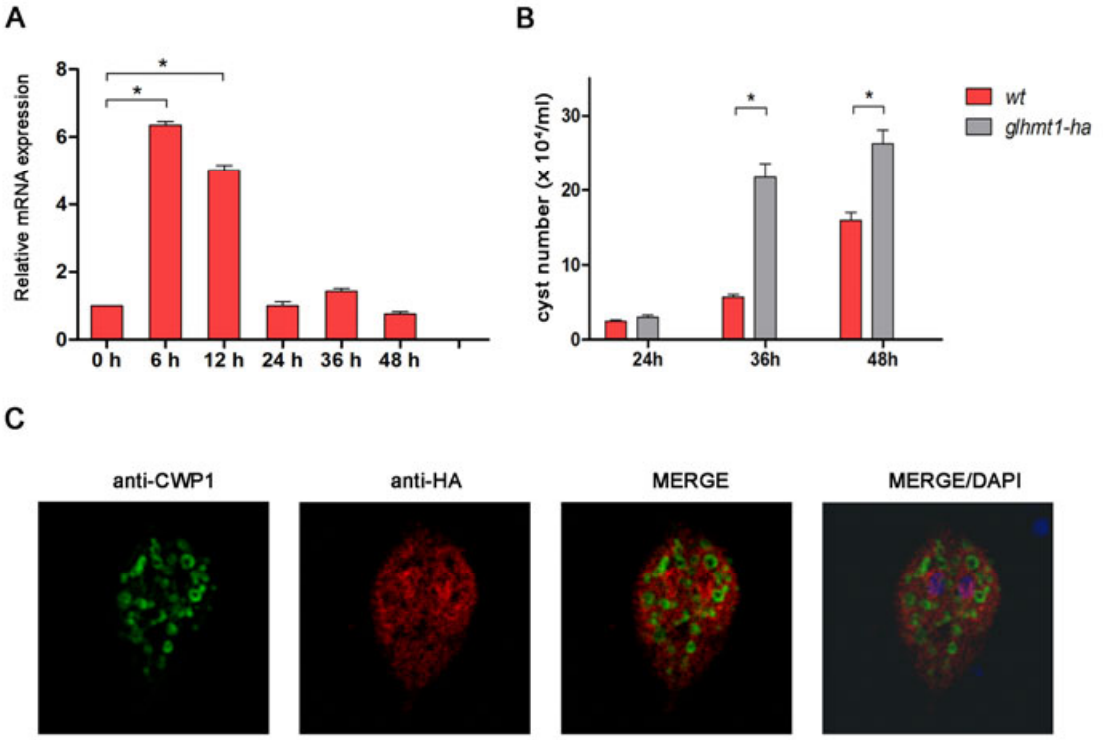

Figure 4. *Giardia* HMT1 during encystation. **A)** Quantitative real time RNA PCR analysis of gene expression in trophozoites from *wt* cells at 0, 6, 12, 24, 36 and 48 h after induction of the encystation process. The assay was performed using primers specific for the *hmt1* gene. Transcript levels were normalized to 18S RNA levels. Fold changes in mRNA expression are shown as the ratio of transcript levels relative to *wt*. **B)** Cyst production analyzed at different times after induction of the encystation process in *wt* and *glhmt1-ha* transfected cells. The number of cysts was significantly higher in *glhmt1-ha* transfected cells compared to *wt* after 36/48 h of encystation. Experiments were repeated at least three times, and data was statistically evaluated using Student's t test, *$p<0.05$. **C)** Immunofluorescence assays and confocal microscopy of *glhmt1-ha* cells during encystation. HMT1-HA proteins were labeled with Texas Red-conjugated anti-HAmAb (red); CWP1 was labeled with FITC-conjugated anti-CWP1mAb (green). Image merging and DAPI staining of the nuclei are shown.

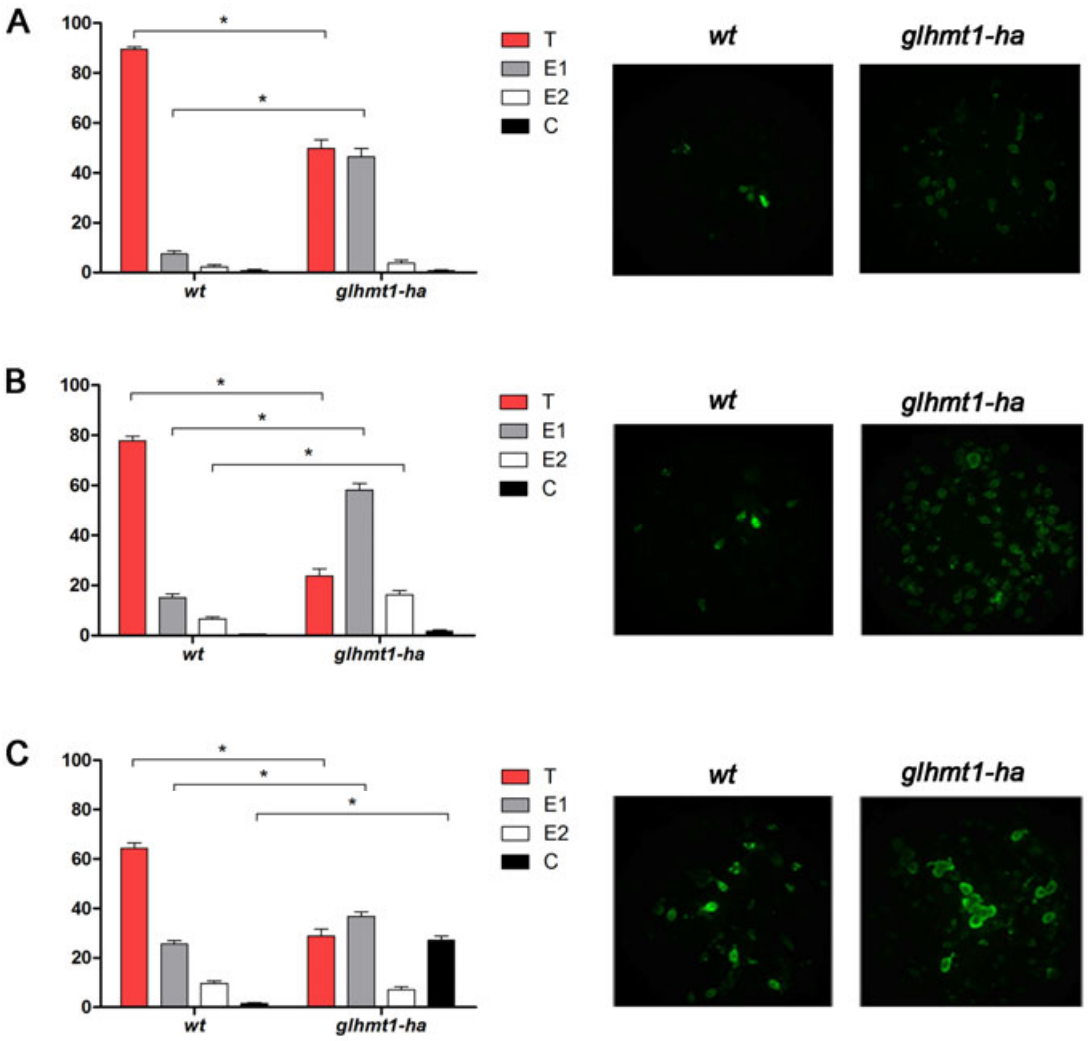

Figure 5. HMT1-HA as an enhancer of the encystation process. Percentage (mean ± SEM) of *wt* and *glhmt1-ha* transfected cells in different encystation stages: trophozoites (T), early encysting (E1), late encysting cells (E2) and cysts (C) were analyzed at different times after encystation induction: **A)** 24 h; **B)** 36 h and **C)** 48 h. Cells were stained with FITC-conjugated anti-CWP1mAb (green) and analyzed by fluorescence microscopy. Right panels represent each time point. Experiments were performed three times and data was statistically evaluated using the Student's t test, *p<0.05.

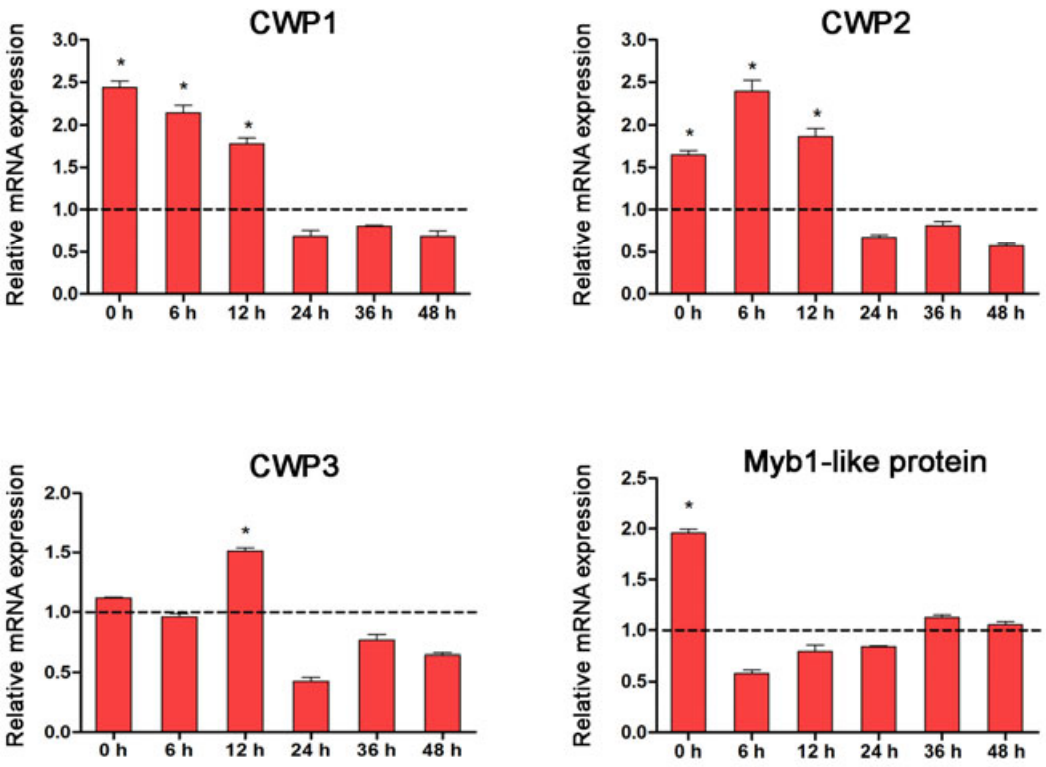

Figure 6. HMT1-HA as a key regulator of the encystation process. Quantitative real time PCR analysis of gene expression in *wt* and *glhmt1-ha* transfected cells at 0, 6, 12, 24, 36 and 48 h after induction of the encystation process. The assay was performed using primers specific for *cwp1*, *cwp2*, *cwp3* and *Myb1-like protein* genes. Transcript levels were normalized to 18S RNA levels. Fold changes in mRNA expression are shown as the ratio of transcript levels in *glhmt1-ha* cells relative to *wt* (dotted line). All experiments were repeated at least three times, and data was statistically evaluated using the Student's t test, *$p<0.05$.

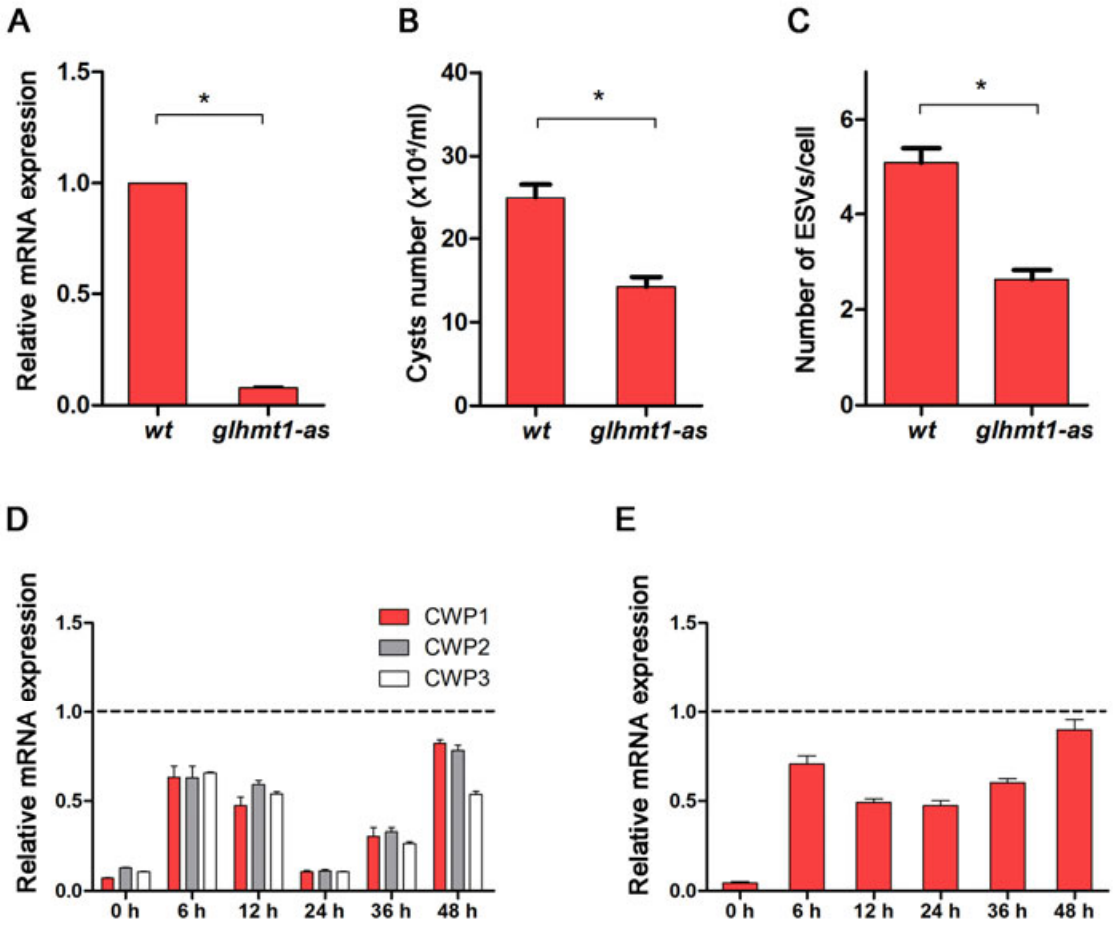

Figure 7. Effect of HMT1-AS downregulation during the encystation process. A) Quantitative real time PCR analysis using *hmt1* gene-specific primers in *wt* and *glhmt1-as* transfected cells showed a reduction in the expression of native hmt1 mRNA in *glhmt1-as* cells at 0 h after induction of the encystation process. **B)** Cyst production was quantified 48 h after induction of the encystation process in *wt* and *glhmt1-as* transfected cells. The number of cysts was significantly lower in *glhmt1-as* transfected cells than in *wt*. **C)** The number of ESVs/cells was counted at 12 h.p.i. of the encystation process in *wt* as well as in *glhmt1-as* transfected cells from three independent experiments. **D-E)** Quantitative real time PCR analysis of gene expression in *wt* and *glhmt1-as* transfected cells at 0, 6, 12, 24, 36 and 48 h after induction of the encystation process. The assay was performed using primers specific for *cwp1-3* gene (D) and m*yb1-like protein* transcription factor gene (E). Transcript levels

were normalized to 18S RNA levels. Fold changes in mRNA expression are shown as the ratio of transcript levels in *glhmt1-as* cells relative to *wt* (dotted lines). All experiments (A-E) were performed at least three times, and data was statistically evaluated using the Student's t test, *$p<0.05$.

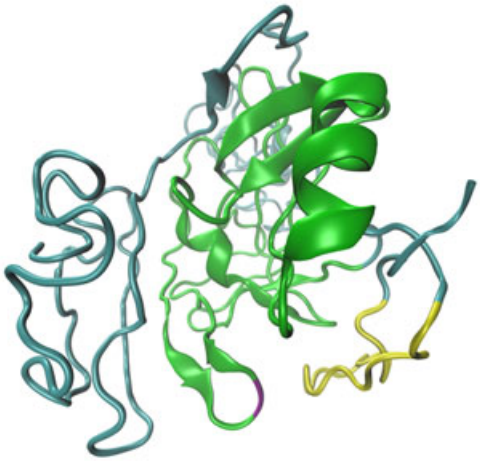

Figure 8. Hypothetical position of K220 within the structure of GlHMT1. In the predicted 3D structure of the protein codified by the gene GL50803_9130 the SET domain (light green), the post-SET domain (yellow) and the exposed K220 (purple) are denoted. Structural analyses were performed using three servers: I-TASSER, Phyre2 and RaptorX. The VMD program was used for visualization of these structures as well as to generate 3D alignment, besides the RaptorX server.